NUCLEAR STRUCTURE--THEORY

SHELL-MODEL CALCULATIONS WITH A SKYRME-TYPE EFFECTIVE INTERACTION

H. Sagawa, B. A. Brown, and O. Scholten

It has been a long-standing problem to establish an effective interaction which can be used both for the calculation of the saturation properties and the excitation spectra of finite nuclei. Vautherin and Brink[1] have proposed a simple interaction, the Skyrme interaction, which has been very successful for Hartree-Fock (H-F) calculations of many nuclei. With a proper parametrization, this interaction gives satisfactory results both for the saturation properties of nuclear matter and the properties of the giant resonances. However, it is not clear whether this interaction is useful also for shell-model calculations of low-lying collective states since most previous parameter sets of the Skyrme interaction such as the SIII set show an anti-pairing effect.[2]

Recently, this problem with the anti-pairing has been improved by the introduction of a density-dependent interaction with a small spin-exchange mixture[3] or the introduction of an additional parameter for the mixing of the density-dependent interaction and the three-body force.[4] The aim of this study is to apply the Skyrme-type interaction to the shell-model calculations of open-shell nuclei and to establish a "universal" effective interaction which can be used for various region of mass table. We use the parameter set SGII[3] in the following calculations as a first attempt. This parameter set reproduces the ground-state properties (the binding energy, the single-particle energies and the root mean square (rms) radius) and also, as will be shown below, the energy spectra. Our calculation is performed in the following way. First, the spherical H-F equation is solved to obtain the single-particle energies (s.p.e.) and radial wave functions. Next, the two-body matrix elements for the SGII interaction are calculated by using these H-F wave functions. Thus, all ingredients of our shell-model calculations are derived from the SGII interaction.

Let us now discuss the shell-model calculations of the s-d shell nuclei. We adopted the experimental s.p.e. for the following open-shell calculations. The results of shell-model calculations for low-lying states of the s-d shell nuclei are shown in Fig. 1. We do not show the excited 0^+ states, such as the state at E_x=3.63 MeV in ^{18}O, which have a large core-excited many-particle many-hole configuration. In Fig. 1, the calculated first 2^+ states both of ^{18}O and ^{36}Ar appear very close to the experimental energies. The first 4^+ and the second 2^+ states are also close to the

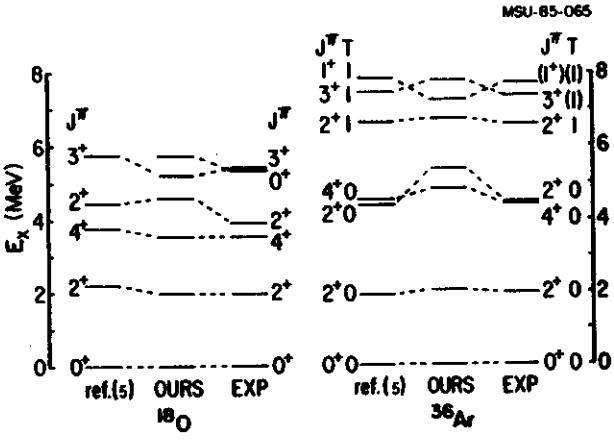

Fig. 1. Calculated and experimental energy spectra of ^{18}O and ^{36}Ar. The data are taken from Ref. 8.

experimental ones. Moreover, the excitation energies of the isovector (T=1) states in ^{36}Ar are also reproduced well. The overall agreement between our calculation and experimental data is almost as good as that obtained by Wildenthal.[5] In the latter case, all two-body matrix elements and single-particle energies are determined by a least square fit to the data, while we have no

free parameter except those in the interaction (1) which has been previously determined.[3]

Arima and his collaborators[6] have claimed that a density-dependent interaction fails to give a realistic spectra at the end of the shell even when it works at the beginning of the shell. However, our interaction gives good agreement in both regions of s-d shell. An important difference between our interaction and that of Ref. (6) is the density dependent term. Since our force has a lower power for the density dependence, the two-body matrix element has a weak mass number dependence. On the other hand, the three-body force (or equivalently a linear power for the density-dependent term) of Ref. (6) has a relatively strong mass dependence and has a much smaller pairing matrix element than ours at the end of the shell.

In order to further investigate the mass dependence, we have also performed the calculations for the Sn-isotopes. Some results are shown in Fig. 2 and compared with

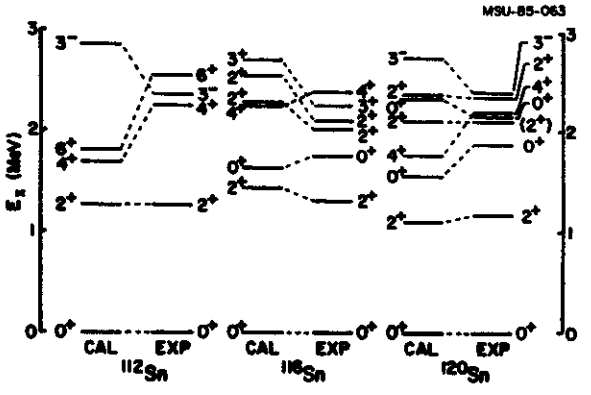

Fig. 2. The energy spectra of Sn-isotopes. The data are taken from Ref. 8.

experimental data. We use the generalized-seniority scheme[7] for these calculations, taking five single-particle states ($3s_{1/2}$, $2d_{3/2}$, $1g_{7/2}$, $1h_{11/2}$ and $2d_{5/2}$) for the neutron configurations. The H-F single-particle energies give the quasi-particle excitations in ^{115}Sn at Ex=0.0 MeV for $3s_{1/2}$, 0.45 MeV for $1g_{7/2}$, 0.52 MeV for $2d_{3/2}$, 1.10 MeV for $1h_{11/2}$ and 1.30 MeV for $2d_{5/2}$, while the experimental ones are 0.0 MeV, 0.61 MeV, 0.50 MeV, 0.71 MeV and 0.99 MeV for these five particle. For the structure calculations discussed below, we have lowered the $h_{11/2}$ s.p.e. by 400 keV. The energy gaps between the 0^+ and 2^+ states are well reproduced by the calculations for all mass numbers. The best agreement occurs in ^{120}Sn where the second and third 0^+ and 2^+ states are also very close to experiment.

Finally, we should notice two shortcomings of our interaction SGII: (1) the relative strengths of the matrix elements for $(1d_{5/2})^2$- and $(1d_{3/2})^2$-multiplets are very close to the phenomenological values, but the absolute magnitudes are larger; (2) our matrix elements for (J=1,T=0) channel and (J=3,T=0) channel of $(1d_{5/2})^2$ configuration differ significantly from those of Wildenthal. As a result of point (1), our calculated ground state binding energies tend to be too large compared to experimental ones. As a result of point (2), the energy spectra of ^{18}F is not as good as those in Fig. 1. We are now attempting to improve these shortcomings and to apply for other mass region.

---

1. D. Vautherin and D.M. Brink, Phys. Rev. C5 626 (1972)
2. L. Zamick, Proc. of Int. Conf. on Nucl. Structure and Spectroscopy, (Amsterdam, 1974) 24.
3. Nguyen van Giai and H. Sagawa, Phys. Lett. 106B, 379 (1981).
4. M. Waroquier et al., Nucl. Phys. A404, 298 (1983).
5. B. H. Wildenthal, Progress in Particle and Nuclear Physics, Vol. II (1983) p.5, and private communications.
6. T. Inoue et al., Proc. of the Int. Conf. on Nucl. Structure, Vol. I (Amsterdam, 1982) p. 318.; A. Arima, Invited talk at Int. Conf. of the Shell Model Theory (Philadelphia, 1984) and private communications.
7. I. Talmi, Nucl. Phys. A172, 1 (1972); O. Scholten, Phys. Rev. C28 (1983) 1783
8. Table of Isotopes (John Wiley & Sons, Inc., 1978) edited by C. M. Lederer and V.S. Shirley)

E2 AND E4 CORE POLARIZATION CHARGES FOR SD-SHELL NUCLEI

H. Sagawa and B. A. Brown

We proposed recently a microscopic model in order to study the core-polarization effect on the transition and current densities of single-particle configurations.[1] This model is essentially made from two parts. At the first stage, we calculate the single-particle wave functions and giant resonances by using the self-consistent Hartree-Fock (H-F) + random phase approximation (RPA) theory. Then, we evaluate the core-polarization effect due to these giant resonances by the particle-vibration coupling model.

In order to calculate E2 core-polarization charges, we have performed the self-consistent RPA calculations of isoscalar (IS) and isovecter (IV) giant resonances in ^{16}O and ^{40}Ca. The obtained excitation energies are close to the experimental ones. Using these results, we calculated core polarization charges for E2 transitions and some results are listed in Table I. The empirical IS and IV effective charge in the mass region A=22-36 have been obtained from a comparison of the experimental E2 matrix elements with those calculated with the full multi-particle $(1d\text{-}2s)^n$ wave functions. The IS empirical effective charge is remarkably state and mass independent with an average value of 0.35±0.05, while the average of the theoretical results (∿0.34) is in excellent agreement with the empirical one. The empirical IV effective charge for the sd-shell nuclei has proved difficult to obtain because it is sensitive to what is assumed for the valence radial wave functions. The present result of +0.11 fits in a range of empirical values from +0.0 to +0.32 obtained by assuming various types of wave functions.[2]

Higher multipole transitions might also give interesting and important information about the nuclear wave functions since they are more sensitive to the radial profiles of the wave functions than the lower multipole transitions,

Table I. IS and IV core polarization charges for E2 transitions in the vicinities of ^{16}O and ^{40}Ca.

f	i	^{16}O		^{40}Ca	
		IS	IV	IS	IV
$1d_{3/2}$	$id_{3/2}$	.17	.07	.40	.11
$1d_{3/2}$	$1d_{5/2}$	.28	.09	.47	.12
$2s_{1/2}$	$1d_{3/2}$	.16	.08	.44	.10
$1d_{5/2}$	$1d_{5/2}$	.36	.10	.42	.12
$2s_{1/2}$	$1d_{5/2}$	.26	.08	.49	.11

especially at the surface region. So far, the E4 transition strengths and the coulomb form factors have been discussed by using s-d shell-model wave functions with phenomenological effective charges[2,3] and also by using the deformed H-F wave functions.[4,5] We will discuss the core-polarization effect on the coulomb E4 form factor in the s-d shell nuclei based on a hybrid microscopic theory which combines shell-model wave functions and highly-excited giant resonances by using the perturbation theory.

The reduced one-body matrix element for shell-model wave functions can be expressed as a linear combination of the single-particle matrix elements;

$$\langle J_f||\hat{T}_\lambda||J_i\rangle = \sum_{\alpha,\beta} C_{J_f,J_i}(\alpha,\beta)\langle\alpha||\hat{T}_\lambda||\beta\rangle \quad (1)$$

where J_f and J_i stand for the shell-model states and $C_{J_f,J_i}(\alpha,\beta)$ are the structure factors (one-body transition densities). The particle-vibration coupling model[1,6] gives the modified single-particle matrix element,

$$\langle\tilde{\alpha}||\hat{T}_\lambda||\beta\rangle = \langle\alpha||\hat{T}_\lambda||\beta\rangle + \sum_{\omega_\lambda}[2\omega_\lambda/(\epsilon^2_{\alpha\beta} - \omega^2_\lambda)] \quad (2)$$

$$*\langle(\beta\times\omega_\lambda)\alpha|V_{ph}|\beta\rangle\langle\omega_\lambda||\hat{T}_\lambda||0\rangle/(2\lambda+1)^{1/2}$$

where ω_λ and $\varepsilon_{\alpha\beta}$ are the excitation energy of giant resonance and single particle energy difference, respectively. The particle-vibration coupling Hamiltonian V_{ph} is derived from the Skyrme-type interaction by replacing the velocity dependent terms by a Fermi-momentum dependent δ-interaction.[1] The modified transition matrix element for the shell-model wave function is now given by inserting $\langle\tilde{\alpha}||\hat{T}||\tilde{\beta}\rangle$ in Eq. (1);

$$\langle\tilde{J}_f||\hat{T}_\lambda||\tilde{J}_i\rangle = \sum_{\alpha,\beta} C_{J_f,J_i}(\alpha,\beta)\langle\tilde{\alpha}||\hat{T}_\lambda||\tilde{\beta}\rangle \qquad (3)$$

This effect can be regarded as a polarization of the core protons by the valence protons and neutrons through the proton-proton and proton-neutron two-body interaction. The proton and neutron core-polarization charges are defined by,

$$\delta e_p = 1 - [\langle\tilde{\alpha}||\hat{T}_\lambda||\tilde{\beta}\rangle_\pi / \langle\alpha||\hat{T}_\lambda||\beta\rangle_\pi]$$
$$\delta e_n = \langle\tilde{\alpha}||\hat{T}_\lambda||\tilde{\beta}\rangle_\nu / \langle\alpha||\hat{T}_\lambda||\beta\rangle_\pi \qquad (4)$$

For the case of the E4 transition, the H-F and RPA calculations have been done first for the hexadecupole giant resonances. The obtained core polarizations are $\delta e(IS)=0.45$ and $\delta e(IV)=0.15$ as averaged values among sd-shell configurations. They are consistent with the empirical effective charges of E4 transitions determined by the comprehensive shell model calculations.[2]

In order to study more details of the wave functions for E4 transitions, the coulomb form factor for the $(0^+ \to 4^+)$ transition in ^{28}Si is shown in Fig. 1. The form factor is increased by a factor of 2.5 at the maximum around q=1.4 fm^{-1}, however, there is not much increase in the high-q region above 2.0 fm^{-1}. This change is attributed to the enhancement of the transition density at the surface region.

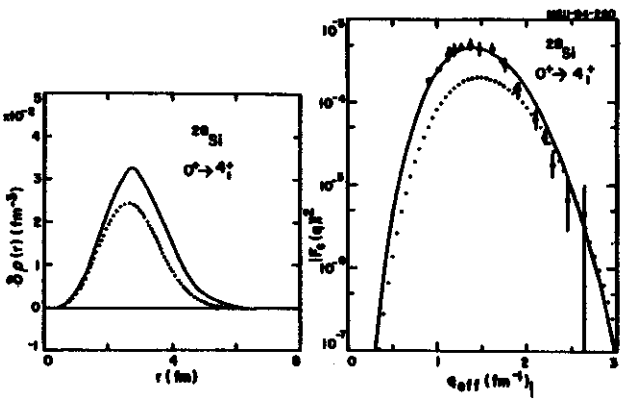

Fig. 1. Transition densities and coulomb form factors for the $(0^+ \to 4^+_1)$ transition in ^{28}Si. The center of mass correction is taken into account in the harmonic oscillator model and the nucleon finite size correction is incorporated in the dipole approximation. The solid and dashed curves correspond to the results with and without core-polarization effects, respectively. The data are taken from Ref. 7.

1. H. Sagawa and B. A. Brown, Nucl. Phys. A430, 84 (1984).
2. B. A. Brown, R. Radhi and B. H. Wildenthal, Phys. Reports C101, 213 (1984).
3. B. A. Brown, W. Chung, B. H. Wildenthal, Phys. Rev. C21, 2600 (1980).
4. L. Zamick, Phys. Lett. 92B, 23 (1980); B. Castel and L. Zamick, Z. Phys. A315, 99 (1984).
5. H. R. Jaqaman and L. Zamick, preprint (RU-10-84, 1984)
6. A. Bohr and B. R. Mottelson, Nuclear Structure, Vol.II (New York, Benjamin, 1979); I. Hamamoto, Phys. Rep. 10C, 1 (1974)
7. R. J. Ryan et al., Phys. Rev. C27, 2515 (1983).

ISOSPIN-MIXING CORRECTIONS TO FERMI DECAYS

W.E. Ormand and B.A. Brown

Superallowed Fermi β-transitions between $J^\pi=0^+$, T=1 analog states have the important feature that since they are purely vector, it is possible to extract from their ft values an accurate determination of the effective vector coupling constant for single nucleon β-decay, provided that nuclear structure corrections to the Fermi matrix element can be properly accounted for. This is important because the difference between this effective vector coupling constant and the coupling constant for the muon decay is dependent on radiative corrections to both decays and the Cabibbo angle. By determining these coupling constants from experimental data, it is possible to test current theories for the radiative corrections and deduce empirical values for the fundamental vector coupling constant and the Cabibbo angle.

For Fermi transitions the relationship between the half-life, vector coupling constant, and the Fermi matrix element is

$$f_R t = \frac{K}{G_V^2 |M_F|^2} \qquad (1)$$

where K is a constant, f_R the statistical rate function, t the partial half-life, G_V the effective vector coupling constant for single nucleon β-decay, and M_F the Fermi matrix element for the transition.

If the initial and final nuclear states are perfect analogs, then the Fermi matrix element is model independent and values for G_V could then be extracted from measured ft values with Eq. (1). The most accurately determined ft values, however, are not constant within experimental uncertainty,[1] suggesting the breaking of analog symmetry between the initial and final nuclei due to the presence of isospin nonconserving (INC) interactions.

We have reexamined these corrections to the Fermi matrix element in the light of recent advances in our understanding of nuclear structure. In particular, wave functions for upper sd-shell nuclei (A=28-39) have been improved with the development of the universal sd-shell (USD) hamiltonian of Wildenthal.[2]

The extent to which analog symmetry is broken is embodied in a correction factor δ_C to the Fermi matrix element defined by $|M_F|^2 = |M_{F0}|^2 (1-\delta_C)$ where M_{F0} is the Fermi matrix element between states with analog symmetry.

The starting point for our calculation of δ_C is the usual spherical shell-model wave functions. Our model space consisted of A-16 nucleons outside an inert ^{16}O core restricted to the 0d1s-shell. Within this basis we need to consider isospin mixing between states within this model space as well as with those outside. Isospin mixing within the model space is calculated by adding the INC interaction onto the isospin-conserving sd-shell hamiltonian, while isospin mixing outside the sd shell is taken into account by allowing the proton radial wave functions to be pushed out relative to the neutron wave functions due to the Coulomb potential. These two effects can be factored[3] into components due to the radial overlaps (RO) and isospin mixing within the configuration space (IM), $\delta_C = \delta_{RO} + \delta_{IM}$.

Previously (Ref. 4), δ_{RO} was evaluated using proton and neutron radial wave functions obtained with a central Woods-Saxon (WS) plus Coulomb potential. This procedure overestimates the difference between the proton and neutron radial wave functions by neglecting an induced isovector interaction that arises from the difference between the proton and neutron densities. To take into account the effects of this induced interaction we have performed self-consistent Hartree-Fock (HF) calculations with a

Skyrme-type interaction (SGII, Ref. 5).

Values of δ_{RO} obtained with the Hartree-Fock wave functions are compared with those of Ref. 4 and are given in Table 1. Values

Table 1. Comparison of the corrections to the Fermi matrix element obtained in the present work and with the values in Refs. 3 and 4. Values of δ are given in %.

Decaying nucleus	Present Work			Previous Values[3,4]		
	δ_{IM}	δ_{RO}	δ_C	δ_{IM}	δ_{RO}	δ_C
^{34}Ar	0.006	0.369	0.375	0.13	0.91	1.04
^{34}Cl	0.056	0.438	0.494	0.23	0.62	0.85
^{30}S	a	0.590	-	0.34	0.87	1.21
^{26}Si	a	0.149	-	0.04	0.38	0.42
^{26}Al	a	0.205	-	0.07	0.27	0.34
^{22}Mg	0.018	0.191	0.209	0.06	0.29	0.35

a) not calculated in the present work

obtained with HF wave functions are systematically reduced relative to those in Ref. 4. This reduction is due to the effects of both the Coulomb and nuclear central potentials used in each calculation. In Hartree-Fock calculations we find that protons are effectively in a potential well which is both deeper at the origin and has a higher barrier at the nuclear surface relative to neutrons. This additional potential tends to draw in the proton radial wave functions relative to the neutrons, and, thus reduce the value of δ_{RO}.

The contribution δ_{IM} was evaluated with isospin-mixed wave functions obtained by adding the INC interaction onto the USD hamiltonian. The one-body transition density (OBTD) matrices for these wave functions were calculated, and δ_{IM} was determined by summing the product of the OBTD matrices and the single-particle matrix elements of the Fermi transition operator. V_{INC} was determined[6] by fitting the three isovector single-particle energies and the parameters of a Coulomb plus phenomenological short-range potential to a set of experimental b- and c-coefficients of the isobaric mass formula.

The isospin mixing corrections to the Fermi matrix elements for ^{22}Mg, ^{34}Cl, and ^{34}Ar are compared with those of Towner and Hardy[3] and are also listed in Table 1. The values of δ_{IM} calculated here are much smaller than those of Towner and Hardy. This difference is due to the zeroth-order wave functions and/or the INC interaction used. The zeroth-order wave functions used in Ref. 3 were obtained with a modified surface delta interaction (MSDI), and the INC interaction was obtained by: (1) adding Coulomb matrix elements to the proton-proton two-body matrix elements, (2) increasing the T=1 part of the MSDI proton-neutron matrix elements by 2%, and (3) using the A=17 energy levels to determine the isovector single-particle energies.

To determine the extent to which the starting wave functions or the INC interactions are responsible for the discrepancy, both the IMME coefficients and δ_{IM} for A=34 were evaluated with all the possible combinations of the isoscalar interaction, isovector single-particle energies, and the two-body INC interaction of the present work and that of Ref. 3. The results of these calculations were that about one-half the discrepancy is explained by different zeroth order wave functions, and that δ_{IM} is strongly sensitive to the isovector single-particle energies. We feel that (1) the USD interaction is more appropriate to determine wave functions for sd-shell nuclei because of the generally better agreement between USD and experimental excitation energies; (2) the isovector single-particle energies determined by the fitting procedure are also more appropriate for the upper sd-shell region because of the loosely bound nature of the A=17 "particle" states.

In the future we hope to evaluate δ_{IM} for

the remaining sd-shell transitions and to extend our method to evaluate δ_C for 0p- and 0f1p-shell superallowed transitions. With these corrections we then hope to determine the effective vector coupling constant G_V with Eq. (1), and to remove the present discrepancy that exists between values of G_V determined from transitions in the fp shell and those determined from the sd-shell transitions.

1. V. T. Koslowsky, Ph. D. Thesis, University of Toronto (1983).
2. B. H. Wildenthal, Progress in Particle and Nuclear Physics, edited by D. H. Wilkinson, (Pergamon Press, Oxford, 1984) Vol.II p.5.
3. I. S. Towner and J. C. Hardy, Nucl. Phys. A205, 33 (1973).
4. I. S. Towner, J. C. Hardy, and M. Harvey, Nucl. Phys. A284, 269 (1977).
5. Nguyen Van Giai and H. Sagawa, Nucl. Phys. A371, 1 (1981).
6. W.E. Ormand and B.A. Brown, Nucl. Phys. A (in press)

CALCULATIONS FOR THE DOUBLE-BETA DECAY OF ^{48}Ca

B. Alex Brown

The study of neutrinoless double-beta decay in nuclei is important for setting limits on the mass and right-handed couplings of the Majorana-type neutrino.[1-3] At first glance the decay of ^{48}Ca is very favorable because of its large decay energy (Q=4.271 MeV) relative to other cases and good experimental limits have been obtained for the decay half-life for both neutrinoless and two-neutrino decay.[4] However, it has become apparent that the nuclear structure matrix elements involved in the decay are quite hindered relative to simple single-particle estimates.[2,5-7] It is important to examine how reliably one can calculate these matrix elements, and we will look at several aspects of this problem and try to arrive at some "best" theoretical values. We note that the single beta decay of ^{48}Ca to ^{48}Sc is allowed (Q=0.281 MeV) but highly forbidden. Warburton[8] has calculated a partial half-life of 7.6×10^{20}y for the unique-fourth-forbidden decay to the 5^+ state at 0.131 MeV and has estimated much longer partial half-lives for the non-unique decays to the 4^+ and 6^+ states.

Double-beta decay may proceed via Fermi or Gamow-Teller type operators.[3] For nuclei with good isospin, the Fermi type operator leads only to the double analog state at 17.38 MeV[9] in ^{48}Ti of the T=4 ^{48}Ca ground state, and the transition to the T=2 ^{48}Ti ground state is forbidden. We have calculated an isospin-mixing matrix element of 26 keV between the T=2 and T=4 states in ^{48}Ti based on the isospin-nonconserving Hamiltonian used in Ref. 10 to describe the displacement energy differences between analog states in this mass region. Using perturbation theory, we find $M_F = \langle 0^+(Ti)||(1/2)\sum_{ij} t_-(i)\, t_-(j)||0^+(Ca)\rangle = 0.005$. M_F is small compared to most of the Gamow-Teller type matrix elements discussed below and can be neglected.

Within the closure approximation,[3] the Gamow-Teller type double-beta matrix elements for two-electron decay have the general form

$$M(DBD) = \langle 0^+(Ti)||O(DBD)F(DBD,r)||0^+(Ca)\rangle \qquad (1)$$

where $O(DBD) = (1/2)O_1(GT-)\cdot O_2(GT-)$
and $O(GT-) = \sum_k \sigma(k)\, t_-(-)(k)$
$r = |\underline{r}(1)-\underline{r}(2)|$ and $t_-|n\rangle = |p\rangle$. We will consider the matrix elements for two-neutrino (2n), light neutrinoless (L), and heavy neutrinoless (H) decay with

$$\begin{aligned} F(2n,r) &= 1 \\ F(L,r) &= 1/r \\ F(H,r) &= \delta(r) \end{aligned} \qquad (2)$$

F(L,r)=1/r is probably a good approximation to a more complicated expression used in Ref. 3. These reduced matrix elements R can be evaluated with shell-model codes such as OXBASH[11] by expanding the matrix element in terms of a sum over products of two-body transition densities (TBTD) times two-body matrix elements (TBME) [Refs. 12 and 13]. The TBME are evaluated with harmonic-oscillator radial wave functions using the Talmi-Moshinsky transformation.[14] We use $\hbar\omega = 45A^{-1/3}-25A^{-2/3}$ MeV.

We have calculated the matrix elements for ^{48}Ca within the $f_{7/2}$ shell-model space using the TBTD calculated with the "^{48}SC" interaction of Ref. 15. The results are very similar to those obtained in Ref. 5 with the "MBZ" interaction of Ref. 16. For 2n DBD the terms in the TBTD expansion nearly exactly cancel. However, the cancellation is smaller for the 0n DBD involving a light neutrino, and there is little cancellation for the 0n decay involving a heavy neutrino. The reason for the cancellation in the case of 2n DBD has been explained in terms of a K-selection rule in the Nilson model.[5]

We can consider an expansion for M(DBD)

involving intermediate states in the ^{48}Sc nucleus. In general, we must sum over all intermediate spins. However, since F(r)=1 for the two-neutrino decay, we need only consider intermediate states in Sc with $J = 1^+$ for this mode, and we can write

$$M(2n) = (1/2)\,\Sigma_m\, M(2n,m) \qquad (3)$$

where $M(2n,m) = M(GT,f,m)\, M(GT,i,m)$ (4)

and $M(GT,k,m) = \langle 0^+(k)||O(GT)||1^+(m)\rangle$ (5)

The Gamow-Teller transition probability for the transition k→m is given by

$$B(GT,k\to M) = M^2(GT,k,m)/(2J_k+1) \qquad (6)$$

These B(GT) obey the sum rule B(GT-)-B(GT+) = 3(N-Z).

In the $f_{7/2}$shell model there is just one intermediate 1^+ state and the DBD could be described diagrammatically as in Fig. 1a below. O(GT) acting on the initial state (Ca) can also go to the $f_{5/2}$ proton configuration as in Fig.1c. This transition is the dominant component of the "giant" GT resonance seen in the ^{48}Ca(p,n) reaction.[17,18] O(GT) acting on the final state (Ti) can also create the pattern in Fig. 1b.

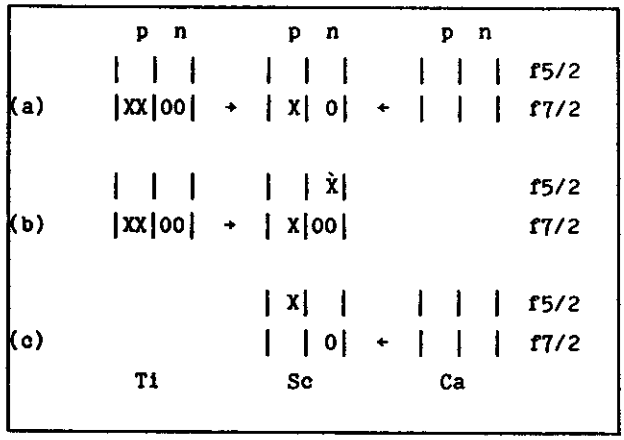

Fig. 1. Schematic diagram for Ca → Ti double-beta decay.

Obviously, only (a) can connect Ti and Ca. However, the intermediate states may be mixed. If only (b) and (c) are mixed and the physical states are $|x\rangle=\alpha|b\rangle+\beta|c\rangle$ and $|y\rangle=\beta|b\rangle-\alpha|c\rangle$ then 2M(2n) is given by

$$\langle f||O(GT)||x\rangle\langle x||O(GT)||i\rangle + \langle f||O(GT)||y\rangle\langle y||O(GT)||i\rangle$$
$$= \alpha\beta\,\langle f||O(GT)||b\rangle\langle c||O(GT)||i\rangle - \alpha\beta\,\langle f||O(GT)||b\rangle\langle c||O(GT)||i\rangle$$

We find two routes each non-zero which cancel. More realistically, all three intermediate states mix, and these also mix with the particle states involving the $p_{3/2}$ and $p_{1/2}$ orbits causing fragmentation. In turn, all of this will be further fragmented by mixing with 2p-2h ... configurations. This pattern of cancellation and fragmentation is in fact found in all of our calculations and can be seen also in Fig. 1 of Ref. 7. Since in the realistic situation the cancellation is not exact and since the $f_{7/2}\to f_{7/2}$ contribution is small, it is important to consider the entire fp shell basis in the double-beta decay calculation.

In Table 1 we give the DBD matrix elements calculated in a 0p0h-1p1h basis relative to a ^{48}Ca closed shell [e.g. the $(f_{7/2})^8 + (f_{7/2})^7(f_{5/2},p_{3/2},p_{1/2})$ configurations] obtained with several recently developed empirical effective interactions. We consider: (1) the interaction of van Hees (VH) from Ref. 19, (2) a modified version of this interaction (MVH) obtained by adding 2 MeV onto the $f_{5/2}$ single-particle energy (Ref. 18), (3) the delta + Yukawa + monopole interaction of Yokoyama (YO) (Ref. 20), and (4) the interaction of Mooy (MO) (Ref. 21). For the MVH interaction we also give the results obtained in the 0p0h-2p2h model space.

This comparison shows the sensitivity of the DBD matrix elements to this aspect of the calculation. However, this does not necessarily

Table 1: Double-beta decay matrix elements calculated with various model spaces and interactions. We also give the summed B(GT) strengths.

Model Space	inter-action	M(2n)	M(L)	M(H)	ΣB(GT,f)	ΣB(GT,i)
0p0h	^{48}Sc	0.194	0.140	0.0127	0.015	10.3
0p0h-1p1h	MVH	-0.056	0.053	0.0095	2.09	22.3
	VH	-0.091	0.045	0.0094	1.94	22.3
	YO	-0.048	0.072	0.0109	2.54	22.3
	MO	-0.226	0.007	0.0082	1.73	22.3
0p0h	MVH	0.249	0.146	0.0124	0.024	10.3
0p0h-1p1h	MVH	-0.056	0.053	0.0095	2.09	22.3
0p0h-2p2h	MVH	0.234	0.163	0.0155	1.77	21.5

mean that the results are uncertain by this amount. We may be able to prefer one interaction over another based on how well it reproduces the experimental energy levels and Gamow-Teller strength functions for nuclei in this mass region. Our investigation of this aspect is at the moment incomplete, but we prefer the "MVH" interaction based primarily on the comparison of the experimental and calculated ^{48}Ca(p,n) Gamow-Teller strength function.[18]

M(2n) is very model-space and interaction dependent and even changes sign when the 1p1h configurations are added. In contrast, the value for M(H) is fairly model independent. The model dependence in M(2n) can be partly understood by looking at the sum in Eq. (3) as a function of excitation energy. As in Fig. 1 of Ref. 7, we find in general that the states just above the first state up to about 6 MeV in excitation (region b) add constructively to the contribution from the first state at 2.52 MeV and that the states above about 6 MeV (region c) add destructively. The breakdown in terms of these three contributions is given in Table 2. The states in region (b) constitute the relatively strong $f_{7/2}$→$f_{5/2}$ transition for the β+ strength (Fig. 1b above) and are relatively weak on the β- side. The reverse is true for the states in region (c).

The double-beta decay matrix elements considered in Eq. (1) are actually approximations to more complex equations involving explicit sums over intermediate states weighted by energy denominators.[3] For two-neutrino decay we should consider the matrix element

$$B(2n) = \Sigma_m \left[Ex(m) + \Delta M + \frac{T_o}{2}\right]^{-1} M(2n,m) \quad (7)$$

where Ex(m) is the excitation energy of the 1^+ state in ^{48}Sc, ΔM=-0.281 is the atomic mass difference and T_o =4.271 MeV is the kinetic energy release. [We assume that this equation is a good approximation to the more exact expression given by Eq.(1) in Ref. 7.] The closure approximation consists in using an average excitation energy <Ex> in the denominator and taking this outside the summation:

$$B^c(2n) = \left[<Ex> + \Delta M + \frac{T_o}{2}\right]^{-1} \Sigma_m M(2n,m) \quad (8)$$

There are many ways in which <Ex> could be estimated, but a common method[3] is to use the β-strength function $M^2(GT,i,m)$ [see Eq. (6)]:

$$\Sigma_m \left[Ex(m) + \Delta M + \frac{T_o}{2}\right]^{-1} M^2(GT,i,m) = \left[<Ex> + \Delta M + \frac{T_o}{2}\right]^{-1} \Sigma_m M^2(GT,i,m) \quad (9)$$

In Table 3 the quantities B(2n) and $B^c(2n)$ are compared. If the closure approximation is valid, they should be about equal. This is certainly not the case, and there is even a change in sign between the two quantities due to the cancellations as a function of excitation

Table 2. M(2n) broken down over regions of excitation energy in ^{48}Sc. Region (a) consists of the first state only. We also give the B(GT) strength to the lowest state at 2.52 MeV (region a).

Model space	inter-action	M(2n) region (a)	M(2n) region (b)	M(2n) region (c)	B(GT,f) region (a)	B(GT,i) region (a)
0p0h-1p1h	MVH	0.171	0.551	-0.778	0.060	1.95
	VH	0.179	0.394	-0.664	0.117	1.09
	YO	0.243	0.253	-0.544	0.056	4.20
	MO	0.101	0.391	-0.718	0.035	1.16
0p0h	MVH	0.249	0	0	0.024	10.3
0p0h-1p1h	MVH	0.171	0.551	-0.778	0.060	1.95
0p0h-2p2h	MVH	0.045	0.743	-0.549	0.076	0.11

Table 3. Comparison of the quantitites B(2n) with those obtained in the closure approximation $B^c(2n)$ using the average excitation energy <Ex> in ^{48}Sc. We also give the summed B(GT) strengths in region (a+b) (see caption to Table 2).

Model space	inter-action	B(2n)	$B^c(2n)$	<Ex>	ΣB(GT,f) region (a+b)	ΣB(GT,i) region (a+b)
0p0h-1p1h	MVH	0.036	-0.006	7.86	1.87	3.39
	VH	0.036	-0.009	7.69	1.82	2.13
	YO	0.043	-0.006	6.48	2.44	6.27
	MO	0.012	-0.022	8.22	1.60	2.11
0p0h	MVH	0.057	0.057	2.52	0.024	10.3
0p0h-1p1h	MVH	0.036	-0.006	7.86	1.87	3.39
0p0h-2p2h	MVH	0.059	0.025	7.81	1.47	4.51

energy discussed in connection with Table 2. We agree with Tsuboi et al.[7] on this point. However, it is encouraging to note that there is less model dependence in the more exact quantity B(2n) than there was in M(2n) [or B^c].

For the neutrinoless double-beta decay there is an additional term of order c/R in the energy denominator which arises from the fact that one of the neutrinos is confined to the region inside the nuclear radius R. Since this number of about 50 MeV is large compared to <Ex>, the closure approximation is better for neutrinoless decay.

Up to now this point we have considered calculations in an fp model space which included up to 2p2h excitation beyond a $f_{7/2}$ closed shell for ^{48}Ca. The largest (J,T) dimensions in this space are 291 for the 0^+ T=2 states. We might consider going up to 3p3h or 4p4h, but calculations in the full fp space (up to 8p8h), where the largest (J,T) dimension is 10872 for the 0^+ T=2 states, is presently impossible. Also, it is important to keep in mind that the effective interactions we use are designed to reproduce energy levels in the 0p0h+1p1h space and that a different interaction might be needed for the full space calculation.

Full space calculations are possible, however, for the sd shell. It is instructive to consider the situation for the nucleus in the sd shell which is most closely analogous to ^{48}Ca, namely ^{22}O, which in the simplest shell model has a $d_{5/2}$ closed-shell configuration for neutrons. In Table 4 we give the results of our calculations for the double-beta decay of ^{22}O obtained with the "USD" interaction of Wildenthal.[22]

The trends in the matrix elements seen in Table 4 on going from the 0p0h to the 0p0h-2p2h model space are very similar to those obtained for the ^{48}Ca matrix elements (see Tables 1 and 3). Therefore, it seems reasonable to use the results of Table 4 to extrapolate the MVH matrix elements for ^{48}Ca to the full fp space. Our algorithm for extrapolation is to multiply the fp shell 0p0h-1p1h MVH values by the ratio of the full-sd over the 0p0h-1p1h values given in Table 4. The results are given in the first

Table 4. Calculated double-beta decay matrix elements for $^{22}O \rightarrow ^{22}Ne$ in the sd shell-model space. For B(2n) and $B^c(2n)$ we use $\Delta M + T_0/2 = 1.854$ MeV. We also give the summed B(GT) strengths in region (a+b).

Model space	B(2n)	$B^c(2n)$	<Ex>	M(L)	M(H)	ΣB(GT,f) region (a+b)	ΣB(GT,i) region (a+b)
0p0h	0.092	0.092	2.52	0.246	0.0181	0.056	6.6
0p0h-1p1h	0.026	-0.012	9.01	0.047	0.0118	0.88	1.48
0p0h-2p2h	0.039	0.011	8.17	0.169	0.0199	0.50	3.68
full sd	0.019	0.0008	9.65	0.135	0.0198	0.28	1.48

line of Table 5.

Our preference for the MVH interaction comes from comparing the B(GT,i) values given in the above Tables with the experimental values obtained from the ^{48}Ca(p,n) reaction:[18,23] 1.31 for region (a) (the state at 2.52 MeV), 2.07 for region (a+b) (the 1^+ states below the IAS), and 9.9-16.2 for the entire spectrum up to 30 MeV in excitation (excluding the T=4 state at 16.8 MeV). The range of values for the entire spectrum depends on whether one includes just the discreet states below 14.5 MeV in excitation (9.9) or adds part of the L=0 continuum (16.2) [see Table I in Ref. 18]. The ratio of experiment over theory is 0.67, 0.61 and 0.43-0.71, respectively. The quenching appears rather uniform in agreement with the systematics obtained for Gamow decays in the sd shell.[24] In terms of this comparison, the second best choice would be the MO interaction of Mooy. However, more comparisons to B(GT) values and energy levels should be made to gain confidence in the reliability of the interactions. In addition, it would be important to have an experimental check on the the ^{48}Ti $\beta+$ strength which might be obtained with the (n,p) or (t,^{3}He) reactions. The theoretical predictions are given by B(GT,f) in Tables 1, 2 and 3 above.

We should also consider the effects of higher-order configuration mixing, delta-isobar admixtures and mesonic exchange currents. These effects (primarily the first two) are responsible for the quenching in the GT strength observed above and in other nuclei.[25] Empirically this quenching is very constant as a function of mass[26] and transition strength[24] with a typical value of 0.60 for the B(GT) values. At a minimum, this quenching should be included in B(2n), and we will also assume it applies to M(L) and M(H) as in the second line of Table 5. The role of these corrections in a more quantitative sense is still a matter of some controversy.[3]

The relationship between the matrix elements considered above and the partial half-lives have the form[3,7,7]

$$T_{1/21/2}(2n) = C(2n)/[B(2n)]^2 \qquad (10)$$

and $$T_{1/2}(0n) = C(L)/[m^2 M(L)]^2 \qquad (11)$$

where m is the mass of the light neutrino. (For simplicity, we assume that the right-handed neutrino couplings vanish.) The statistical and phase-space factor $C(2n)=2.3\times10^{16}$y deduced from Ref. 7 is consistent with Ref. 3. From Ref. 3 we obtain $C(L)=420\times10^{20}(eV)^2$y. For our comparison in Table 5, we take the value m=31 eV suggested from a recent measurement of the end-point spectrum of the beta decay of tritium.[27] We will not discuss the neutrinoless decay involving heavy (H) virtual neutrinos here. The comparison with experiment in Table 5 suggests that it would be interesting to push these experimental limits an order of magnitude further.

Table 5. Final results for the ^{48}Ca two-neutrino (2n) and neutrinoless (0n) double-beta decay.

Matrix elements	B(2n)	M(L)	M(H)
Extrapolated fp	0.026	0.152	0.0159
Extrapolated fp times 0.60 quenching	0.016	0.091	0.0096

Partial Half-life	$T_{1/2}(2n)$	$T_{1/2}(0n)$ in units of 10^{20}y	
Calculated	0.9	53*	
Experimental	>0.36	>20	(Ref. 4)

*Assuming 31 eV for the light Majorana neutrino mass and vanishing right-handed couplings.

1. H. Primakoff and S.P. Rosen, Ann. Rev. Nuc. Part. Sci. 31, 145 (1981).
2. W.C. Haxton, G.J. Stephenson, and D. Strottman, Phys. Rev. Lett. 47, 153 (1981) and Phys. Rev. D25, 2360 (1982).
3. W.C. Haxton and G.J. Stephenson preprint submitted to Progress in Particle and Nuclear Physics.
4. R.K. Bardin, P.J. Gollon, J.D. Ullman, and C.S. Wu, Nucl. Phys. A158, 337 (1970).
5. L. Zamick and N. Auerbach, Phys. Rev. C26, 2185 (1982).
6. L.D. Skouras and J.D. Vergados, Phys. Rev. C28, 2122 (1983); and J.D. Vergados, Phys. Rev. C13, 865 (1976).
7. T. Tsuboi, K. Muto and H. Horie, Phys. Lett. 143B, 293 (1984).
8. E.K. Warburton, preprint submitted to Phys. Rev. C (1985).
9. R.T. Kouzes, . Kutt, D. Mueller, and R. Sherr, Nucl. Phys. QA309, 329 (1978).
10. B.A. Brown and R. Sherr, Nucl. Phys. A322, 61, (1979).
11. W.M.D. Rae, A. Etchegoyen, N.S. Godwin, and B.A. Brown, The Oxford-Buesnos Aires Shell Model Code, unpublished.
12. P.J. Bussaard and P.W.M. Glaudemans, Shell Model Applications in Nuclear Spectroscopy (North Holland, Amsterdam, 1977).
13. B.A. Brown, W.A. Richter, and N.S. Godwin, Phys.Rev. Lett. 45, 1681 (1980).
14. I. Talmi, Helv. Phys. Acta 25, 185 (1952); and M. Moshinsky, Nucl. Phys. 13, 104 (1959).
15. W. Kutschera, B.A. Brown, and K. Ogawa, Rivista del Nuovo Cimento, Serie 3, Vol. 1 No. 12 (1978).
16. J.D. McCullen, B.F. Bayman and L. Zamick, Phys.Rev. 134B, 515 (1964).
17. B.D. Anderson, J.N. Knudson, P.C. Tandy, J.W. Watson, R. Madey, and C.C. Foster, Phys. Rev. Lett. 45, 699 (1980).
18. B.D. Anderson, T. Chittrakarn, A.R. Baldwin, C. Lebo, R. Madey, J.W. Watson, B.A. Brown, and C.C. Foster, Phys. Rev. C31, 1161 (1985).
19. A.G.M. van Hees and P.W.M. Galudemans, Z. Phys. A303, 267 (1981).
20. A. Yokoyama, T. Oda, and H. Horie, Phys. Rev. C31, 1013 (1985) and private communication.
21. R.B.M. Mooy and P.W.M. Glaudemans, Z. Phys. A312, 59 (1983) and private communication.
22. B.H. Wildenthal, Lectures presented at the International School on Nuclear Physics; 7th course: Mesons, Quarks and Nuclear Excitations, Erice-Trapany-Sicily, 6-18 April 1983, Progress in Particle and Nuclear Physics, Vol. 11, p. 5.
23. B.D. Anderson, private communication.
24. B.A. Brown and B.H. Wildenthal, Phys. Rev. C28, 2397 (1983) and submitted to Atomic and Nuclear Data Tables.
25. I.S. Towner and F.C. Khanna, Nucl. Phys. A399, 334 (1983).
26. C.D. Goodman et al., Phys. Rev. Lett. 44, 1755 (1980) and C.D. Goodman, Proceedings of the International Conference on Nuclear Physics (Tipografia Compositori, Bologna) edited by B. Blasi and R.A. Ricci, Vol. 2 (1983) p. 165.
27. S. Boris et al., paper presented at HEP 83, Brighton (July 1983).

DOUBLE BETA DECAY IN MEDIUM HEAVY NUCLEI

O. Scholten and Zurong Yu

The double beta decay process is of much interest because it probes lepton conservation.[1] One important ingredient of the calculation is the nuclear many body matrix element. This matrix element has been calculated by Haxton[2] in the shell-model. While for lighter nuclei these calculations and experiment are roughly in agreement, for heavy nuclei the discrepancy is in most cases larger than a factor 5. It has been shown[3] that nuclear deformation tends to suppress the double-beta decay rate. In order to be able to include these deformation effects, we have performed the calculation in the framework of the IBA model.

The operator that describes L=0 double beta decay for the nuclei we are interested in is

$$O^{B}_{2\beta} = A(s^{\dagger}_{\pi}\cdot s^{\dagger}_{\nu})+B(d^{\dagger}_{\pi}\cdot d^{\dagger}_{\nu})+C(s^{\dagger}_{\pi}s^{\dagger}_{\pi}s^{\dagger}_{\nu}s^{\dagger}_{\nu}\tilde{d}_{\pi}\cdot\tilde{d}_{\nu})/(Z_{\pi}Z_{\nu}) + E_{\pi}(s^{\dagger}_{\pi}s^{\dagger}_{\pi}\tilde{d}_{\pi}\cdot d^{\dagger}_{\nu})/Z_{\pi} + E_{\nu}(s^{\dagger}_{\nu}s^{\dagger}_{\nu}d^{\dagger}_{\pi}\cdot\tilde{d}_{\nu})/Z_{\nu} \qquad (1)$$

$$Z_{\rho} = \sqrt{N_{\rho}(N_{\rho}-1)}\ ,\ \rho = \pi,\nu \qquad (2)$$

The parameters A-E can be calculated using the OAI[4] mapping procedure. The equivalent fermion matrix elements can be calculated using the generalized seniority model.[5] The parameters of the shell model hamiltonian have been adjusted to reproduce the spectra of the nearby semi-closed shell nuclei. The resulting values for the A and B coefficients are given in Table 1. It should be noticed that in general B has the opposite sign from A, which means that in the calculation of the double beta decay, the first and the second term in (1) interfere destructively, i.e. the presence of d-bosons (deformation) decreases the double beta decay rate, in accordance with the results given in Ref. 3. The calculated matrix elements are compared with the results of Haxton[2] and experiment in Table 2. It can be seen that there is still a discrepancy left, which might be related to the usage of the closure relation in the evaluation of the double beta decay matrix elements.

Table 1. The calculated values for the coefficients in the boson image of the double beta decay operator, Eq. (1). Also the expectation value of the boson operators multiplying these coefficients is given.

Decays	A	B	C	E_{π}	E_{ν}
$^{128}Te \rightarrow ^{128}Xe$	.848	-.402	-.007	.041	.145
boson m.e.	2.20	1.18	1.19	0.19	0.33
$^{130}Te \rightarrow ^{130}Xe$	.900	-.436	-.005	.039	.117
boson m.e.	2.20	1.12	0.49	0.05	0.06

Table 2. The calculated and experimental double Gamow-Teller matrix elements.

Decays	$\lvert M_{GT}\rvert_{IBA}$	$\lvert M_{GT}\rvert_{Haxton^2}$	$\lvert M_{GT}\rvert^{*}_{exp}$
$^{128}Te \rightarrow ^{128}Xe$	1.44	1.47	0.185-0.230
$^{130}Te \rightarrow ^{130}Xe$	1.49	1.48	0.104-0.129

*Taken from Ref. 2.

1. W.C. Haxton, G.J. Stephenson, Jr., and D. Strottman, Phys. Rev. Lett. 47, 153 (1981).
2. W.C. Haxton, G.J. Stephenson, Jr., and D. Strottman, Phys. Rev. D25, 2360 (1982); D26, 1805 (1982); W.C. Haxton, G.A. Cowan, and M. Goldhaber, Phys. Rev. C28, 467 (1983); W.C. Haxton and G.J. Stephenson, Jr., Phys Rev. C28, 456 (1983).
3. L. Zamick and N. Auerbach, Phys. Rev. C26, 2185 (1982).
4. T. Otsuka, A. Arima and F. Iachello, Nucl. Phys. A309, 1 (1978).
5. O. Scholten, Phys. Rev. C28, 1783 (1983).

GENERALIZED SENIORITY IN THE PRESENCE OF STRONG SHELL EFFECTS

O. Scholten, S. Pittel,* and T. Otsuka**

Recently, interest in generalized seniority[1] has been rekindled by the phenomenological success of the Interacting Boson Model (IBM). Generalized seniority provides a natural microscopic framework in which to derive the IBM in near vibrational nuclei. For this reason we have investigated generalized seniority not as an exact symmetry, but rather as an approximate symmetry which can be used to formulate a meaningful variational approach.

In such an approach, the ground state of a system of 2N valence nucleons (of a given type) is described by a generalized seniority v=0 variational ansatz of the form

$$|S^N\rangle = \eta(S^\dagger)^N|\bar{0}\rangle \qquad (2)$$

where

$$S^\dagger = \sum_j \alpha_j S_j^\dagger \qquad (3)$$

$$S_j^\dagger = \sqrt{\frac{j+1/2}{2}} \quad [a_j^\dagger a_j^\dagger]^{(0)} \qquad (4)$$

$a_j^\dagger$ creates a nucleon in orbit j, $|\bar{0}\rangle$ denotes the inert core and η is a normalization constant. The coefficients α_j are treated as variational parameters, determined by minimizing the expectation value of the hamiltonian.[2] An interesting and still unresolved issue is whether generalized seniority can provide an acceptable variational approximation to low-lying states in the presence of strong shell effects. A characteristic feature to be expected when shell effects dominate, is a discontinuity in two-nucleon separation energies at the "shell closure".

To address the usefulness of generalized seniority in the presence of shell effects, we have studied a schematic problem involving two shells, each degenerate but split with respect to one another. The active orbits are

(i) those from the 50-82 major shell (denoted shell 1), which we assume to be degenerate and

(ii) the $1h_{9/2}$ orbit (denoted shell 2), which we assume to be at energy Δ above the orbits in shell 1.

We consider the problem of N active nucleon pairs interacting through a Surface Delta Interaction (SDI)[3] with strength g=0.2 MeV. We have carried out variational calculations for the generalized seniority ansatz (2-4) for several values of the shell splitting Δ and for several nuclei near the N=16 closure of shell 1. The variational minimizations were achieved using the iterative diagonalization procedure of Ref. 2. The resulting ground state binding energies are presented in Table 1, in the column denoted GS (for generalized seniority).

The Hamiltonian can in principle couple the variational ground state to v=4 states. A measure of the extent of this coupling and thus the extent to which the variational solution is not an eigenstate of the hamiltonian is provided by the fluctuation energy $\sqrt{\langle H^2\rangle - \langle H\rangle^2}$, which we also present in Table 1.

Table 1. Ground State Binding Energies and Fluctuation Energies for Generalized Seniority Calculations

N	Δ	GS	$\langle H^2\rangle - \langle H\rangle^2$
14	0	58.8	0.0
15		63.0	0.0
16		67.2	0.0
17		71.4	0.0
18		75.6	0.0
14	2	49.26	0.27
15		52.40	0.31
16		55.41	0.30
17		58.27	0.23
18		60.96	0.13
14	4	46.39	1.56
15		49.27	2.11
16		51.97	2.93
17		51.68	1.45
18		51.09	0.62

The relevant dimensionless parameter that determines whether we are in an interaction-dominated or a single-particle-splitting-dominated regime is $\Delta/\bar{\Omega}g$ where $\bar{\Omega} = \sqrt{\Omega_1\Omega_2} \sim 9$. Thus, for Δ=0 MeV the interaction dominates, for Δ=2 MeV the interaction and single-particle splitting are of comparable importance and for Δ=4 MeV the single-particle splitting (or shell effect) dominates.

Since the centroid of the states left out from the variational basis lies around an excitation energy of 2Δ, it can be checked from Table 1 that the generalized seniority ansatz provides indeed a valid variational wave function.

* Bartol Research Foundation.
** J.A.E.R.I., Tokai, Japan

1. I. Talmi, Nucl. Phys. A173, 1 (1971).
2. O. Scholten, Phys. Rev. C28, 1783 (1983).
3. I.M. Green and S.A. Moszkowski, Phys. Rev. 139B, 790 (1965).

FORM FACTORS IN IBA

O. Scholten, H. Sagawa, and B.A. Brown

Form factors have been calculated in the IBA-model using a semi-phenomenologic approach. In IBA the E2 transition densities, for example, can be calculated from

$$\rho^{E2}(r) = \alpha(r)(s^{\dagger}\tilde{d}+d^{\dagger}s)^{(2)}+\beta(r)(d^{\dagger}\tilde{d})^{(2)}. \quad (1)$$

The matrix elements of the boson operators in Eq. (1) can be evaluated from the IBA wave functions of the states involved. The functions $\alpha(r)$ and $\beta(r)$ can be determined from the observed transition densities to two states, and other transition densities can subsequently be predicted.[1]

We have performed a microscopic calculation of the basic boson transition densities $\alpha(r)$ and $\beta(r)$. There are two contributions to these densities, one arising from the nucleons in the valence shell and one from excitations outside this space, i.e. core polarization. We will discuss here the results for the nucleus ^{110}Pd.

The valence space contribution is calculated in the generalized seniority model which is discussed extensively in Ref. 2. The parameters for the fermion hamiltonian have been obtained from a fit to the semiclosed shell Sn isotopes and the N=50 isotopes. The calculated densities $\alpha(r)$ and $\beta(r)$ are shown in Fig. 1. If no core-polarization contribution is added, there are two major differences with experiment,[3] (i) the boson effective charge (the integrated density $\alpha(r)$) is about 50% too small, and (ii) the experimentally established peaking of the transition density of the surface is not reproduced. These two discrepancies can be resolved by including core-polarization effects in the calculation.

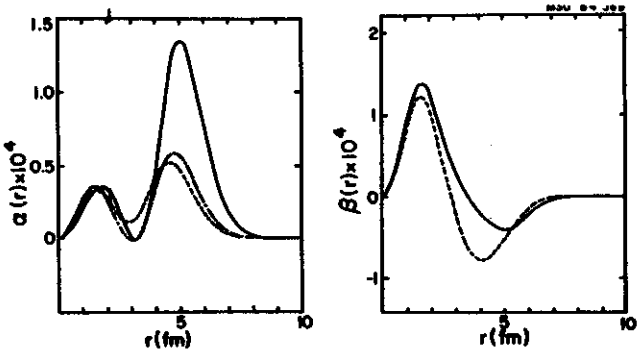

Fig. 1. The calculated transition densities $\alpha(r)$ and $\beta(r)$. The dashed curves represent the results of the calculation in the absence of core polarization. The drawn curves give the result when core polarization is included.

The core polarization is calculated by considering the admixtures of the quadrupole giant resonances in the low lying states using perturbation theory. The giant resonance spectrum is calculated from an RPA calculation.[4] The $2\hbar\omega$ resonance around 20 MeV excitation gives the dominant contribution. Since the transition density of this state is strongly surface peaked, the effect of the core polarization is to enhance the surface peak, bringing it closer in agreement with the data.

1. A.E.L. Dieperink, Nucl. Phys. A358, 189c (1981).
2. O. Scholten, Phys. Rev. C28, 1783 (1983).
3. C.W. de Jager, Interacting Boson-Boson and Boson-Fermion Systems, ed. O. Scholten (World Scientific, 1984) p. 225.
4. N. van Giai and H. Sagawa, Phys. Lett. 106B, 379 (1981).

LOW LYING MIXED SYMMETRY K=0 BANDS IN DEFORMED NUCLEI

O. Scholten, K. Heyde,* and T. Otsuka**

Recently the states of mixed neutron-proton symmetry, as predicted by the IBA model, have drawn much interest with the discovery[1] of the collective $K=1^+$ bandhead. In the deformed rare earth nuclei this state lies at an excitation energy of about 3 MeV. Of particular importance in studying the states of mixed neutron-proton symmetry, is the Majorana force in the IBA-2 hamiltonian,

$$M_{\nu\pi} = \xi_2(s_\nu^\dagger d_\pi^\dagger - d_\nu^\dagger s_\pi^\dagger)^{(2)}\cdot(s_\nu \tilde{d}_\pi - \tilde{d}_\nu s_\pi)^{(2)} - 2\sum_{k=1,3}\xi_k(d_\nu^\dagger d_\pi^\dagger)^{(k)}\cdot(\tilde{d}_\nu \tilde{d}_\pi)^{(k)}$$

The conventional choice for the parameters is $\xi_1=\xi_2=\xi_3=a$. When a is chosen so as to put the $K=1^+$ band in deformed nuclei at $E_x = 3$ MeV (a=0.2 MeV) all other mixed symmetry states lie also at this energy or higher. This has lead one to believe that all mixed symmetry states in deformed nuclei lie above 3 MeV excitation energy. We have investigated another equally plausible choice for the parameters in the Majorana force, namely $\xi_1=\xi_3=b$ and $\xi_2=0$. For b=0.3 MeV the $K=1^+$ band lies also at 3 MeV, but there are some interesting differences in the spectrum. The most striking feature in the spectrum (see Fig. 1) is the occurrence of a relatively low-lying $K=0^+$ band of mixed symmetry. This band is close in energy to an observed $K=0_3^+$ band which lies near the β-band. This band has been interpreted as a two quasi-particle band on the basis of E2 transitions, which are less than 1 s.p.u., and on the basis of (p,t) and (t,p) cross sections.[2] The properties of this mixed symmetry $K=0^+$ band appear to be identical thus leaving the possibility wide open to interpret the $K=0_3^+$ band not as a 2 q.p. state, but rather as the long sought $k=0^+$ mixed symmetry band.

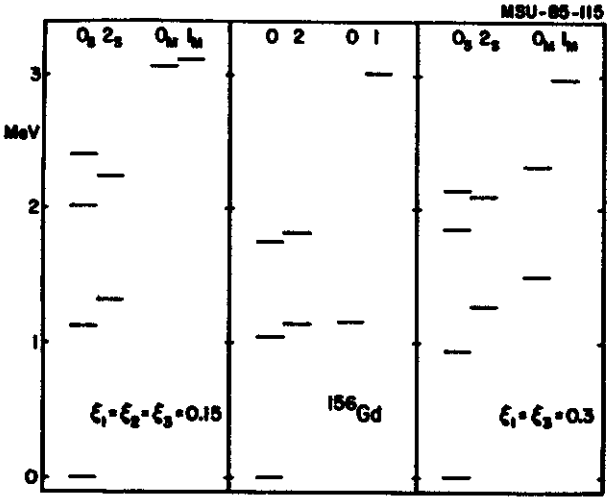

Fig. 1. Calculated positions of the bandheads in a typical deformed rare earth nucleus using the two different choices for the Majorana operator, as discussed in the text.

* R.U., Gent, Belgium.
** J.A.E.R.I., Tokai, Japan

1. D. Bohle, et al., Phys. Lett. 137B, 27 (1984); Phys. Lett. 148B, 260 (1984).
2. A. Bohr and B.R. Mottelson, Nuclear Structure, vol. 2 (Benjamin, New York, 1975); V.G. Soloviev, Dubna preprint E4-84-602 (1984).

THE BASIS FOR SYMMETRIC IRREDUCIBLE REPRESENTATION OF SO(9)×SU(1,1) AND THE INTERACTING BOSON MODEL

Z.R. Yu, O. Scholten and H.Z. Sun*

For the n g-bosons system, we have constructed a set of basis wave function by means of the direct product group SO(9)×SU(1,1) and the subgroup chain

$$SO(9) \supset SO(5)\times SU_1(2)\times SU_2(2).$$

The branching rule of $SO(9)\supset SO(5)\times SU_1(2)\times SU_2(2)$ can be derived by means of Shur function method.[1,2] It can be written as follows

$$(v0000)\supset((p,0),\ \tfrac{1}{2}\Sigma,\ \tfrac{1}{2}\Sigma) \qquad (1a)$$

where v is the seniority quantum number, $\Sigma=v-p-2\omega$, and

$$p = 0,1,2,\ldots,v;\quad \omega = 0,1,2,\ldots,\left[\tfrac{v-p}{2}\right] \qquad (1b)$$

Symbol $\left[\frac{v-p}{2}\right]$ stands for the maximum integral of $\frac{v-p}{2}$.

For the quasi-spin boson group SU(1,1), its generators read

$$\hat{S}_+ = \tfrac{1}{2}\, g^\dagger\cdot g^\dagger,\quad \hat{S}_- = \tfrac{1}{2}\,\tilde{g}\cdot\tilde{g},\quad \hat{S}_0 = -\tfrac{1}{2}\,(\hat{N}+\tfrac{9}{2}) \qquad (2)$$

where $g^\dagger(\tilde{g})$ is a creation (annihilation) operator, and $\hat{N}$ is the boson number operator. Their commutation relations are well known. The quantum numbers

$$S = \tfrac{1}{2}(v+\tfrac{9}{2}),\quad S_0 = \tfrac{1}{2}(n+\tfrac{9}{2})\quad v=n,n-2,\ldots,1\text{ or }0$$

distinguish the states of different irreps. The relation (3) shows the known connection between the irrep of SO(9) and SU(1,1). Hence, a general state vector for the symmetric irrep of SO(9)×SU(1,1) can be written as $|\phi\rangle=|nv\Omega\rangle$. Here Ω is the total quantum numbers which label the irreps of the groups $SO(5), SU_1(2), SU_2(2)$ and their subgroups.

For convenience of construction of the state vector $|nv\Omega\rangle$, we introduce a set of new generators for the group chain $SO(9)\supset SO(5)\times SU_1(2)\times SU_2(2)$, as follows

$$\hat{\chi}_{\mu\nu} = g^\dagger_\mu \tilde{g}_\nu - g^\dagger_\nu \tilde{g}_\mu ,\quad \mu,\nu = 0,\pm1,\ldots,\pm4 \qquad (4)$$

The connection between $\hat{\chi}_{\mu\nu}$ and the generators of SO(9) in the IBM is

$$(g^\dagger\tilde{g})^k = \tfrac{1}{2}\sum_{\mu\nu} C^{kq}_{4_\mu 4_\nu}\,\chi_{\mu\nu}\quad k=1,3,5,7;q=0,1,\ldots,k \qquad (5)$$

Using $\hat{\chi}_{\mu\nu}$ we can easily construct the generators of the subgroups SO(5), $SU_1(2)$ and $SU_2(2)$ and the Casimir operator of SO(9) in the IBM.

Finally, we may obtain a general state, as follows

$$|nv;p,\Lambda\alpha\beta,\Sigma\gamma\delta\rangle = \sqrt{\frac{(2v+7)!!}{2^\rho\rho!(2\rho+2v+7)!!}}\,(S_+)^\rho|vv;p,\Lambda\alpha\beta,\Sigma\gamma\delta \qquad (6)$$

where $\rho=(n-v)/2\cdot p,\Lambda,\Sigma$, etc., are the irrep labelings of the groups SO(5), $SU_1(2)$, $SU_2(2)$ and their subgroups, respectively.

Equation (6) gives only the mathematical basis. The physical basis can in principle be obtained in terms of projection technique. However, if we would have chosen a reduction of SO(9) into SO(3), there would have been several missing labels, for which it is extremely difficult (impossible) to find a simple physical interpretation. For this reason we prefer the reduction scheme outlined in this paper.

---

* Drexel University

1. B.G. Wybourne, Classical Groups for Physicists, 1974.
2. R.C. King, J. Phys. A. Math. Gen. 8, 429 (1975).

ON THE RELATION BETWEEN THE IBFA MODEL AND DYNAMICAL BOSON-FERMION SYMMETRIES

R. Bijker* and O. Scholten

In the extension of the IBA model to odd-mass nuclei by coupling the single particle (fermion) degrees of freedom to the collective (boson) degrees of freedom of the core nucleus, two basically different approaches are possible. In one approach[1] the structure of the boson-fermion interaction is constructed entirely on the basis of group-theoretical arguments, such that the hamiltonian exhibits a dynamical symmetry. In this case the full spectrum can be calculated analytically and a simple labeling system for the levels is obtained. This has contributed significantly to the insight in the structure of the complicated odd-mass spectra. Several examples of these symmetries have been found in the spectra of odd-even nuclei.[1] In a different approach, the Interacting Boson Fermion Approximation (IBFA),[2] the structure of the boson-fermion interaction is derived using a semi-microscopic theory.[3] The question now arises how the IBFA and the symmetry approach, describing the structure of odd-mass nuclei, are related to each other.

We have studied this relation in the case of the SO(6)⊗U(2) limit of the IBFM. By equating the coefficient of the corresponding terms in the boson-fermion interaction, we obtain a relation between the coefficients, which is shown in Figs. 1 and 2. In these figures ν_0, Γ_0, Λ_0, χ and E are parameters of the IBFA hamiltonian, while β, η, γ and ζ appear in the boson-fermion symmetry description. An extensive discussion of the details is given in Ref. 4.

On the basis of this relation, definite predictions are obtained as to where the SO(6)⊗U(2) symmetry can be expected to occur, i.e. in which nuclei. One region is the odd-neutron isotopes of Kr-Sr and another is formed by odd-neutron isotopes of Pt and Os near A≈195. The predictions following from this relation

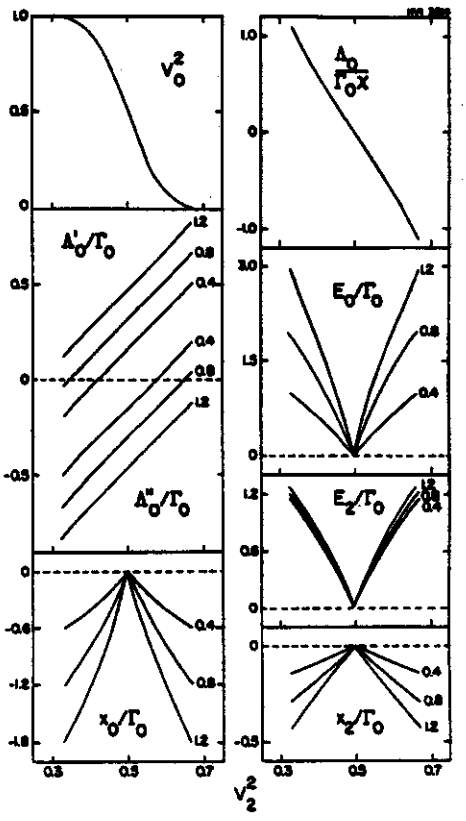

Fig. 1. Ratios of IBFA parameters as a function of v_2^2 for three different values of $|\chi|$=0.4, 0.8 and 1.2

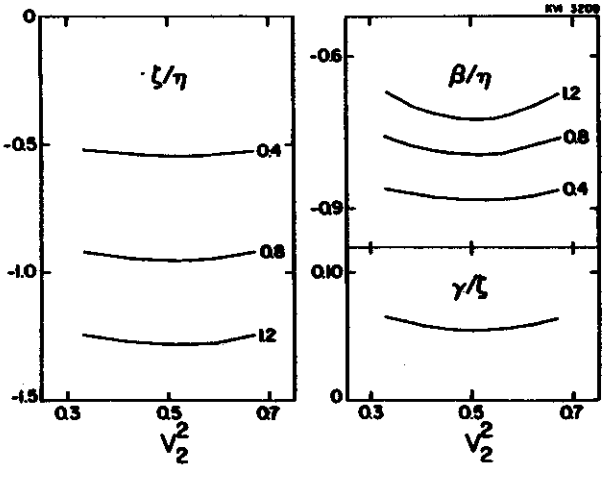

Fig. 2. Ratios of parameters in the SO(6)×U(2) limit as a function of v_2^2 for three different values of $|\chi|$=0.4, 0.8 and 1.2.

between the two models agree rather well with phenomenology. The spectrum of ^{195}Pt, for example, has been calculated before in the boson-fermion symmetry model,[5] using as parameters $\beta/\eta=-1.05$, $\gamma/\xi=-.08$ and $\xi/\eta=-1.9$ with $|\chi|=0.8$, which are in good agreement with the values that can be read from Fig. 2.

---

* University of Pennsylvania.

1. R. Bijker and V.K.B. Kota, Ann. Phys. (N.Y.) 156, 110 (1984); P. van Isacker, A. Frank, and H.Z. Sun, Ann. Phys. (N.Y.) 157, 183 (1984); R. Bijker and F. Iachello, Ann. Phys. (N.Y.), to be published; and references therein.
2. F. Iachello and O. Scholten, Phys. Rev. Lett. 43, 679 (1979).
3. O. Scholten, Ph.D. thesis, University of Groningen, 1980; O. Scholten and A.E.L. Dieperink, in Interacting Bose-Fermi Systems in Nuclei, F. Iachello, ed., Plenum Press, N.Y. (1981) 343.
4. R. Bijker and O. Scholten, preprint MSUCL-508 (1985).
5. H.Z. Sun, A. Frank and P. van Isacker, Phys. Rev. C27, 2430 (1983); R. Bijker, Ph.D. thesis, University of Groningen, 1984.

M1 TRANSITIONS IN THE IBA MODEL

O. Scholten, A.E.L. Dieperink*, and D. Warner**

In view of the recent discovery of mixed symmetry states in the spectra of deformed rare earth nuclei,[1] as predicted by IBA,[2] it is interesting to obtain a measure for the amount of mixing of the symmetric and mixed symmetry states. M1 transition probabilities are a particularly sensitive probe for this. The M1 transition matrix elements vanish identically for states that are fully symmetric in the neutron and proton degrees of freedom. In the model M1 transitions between low-lying, predominantly symmetric states do only occur via the small mixed symmetry components that are admixed.

On the basis that the admixtures of mixed symmetry components are small, we have done perturbation theory calculations to obtain quantitative expressions for the mixing. This mixing will depend on the strength of the symmetry breaking terms in the hamiltonian. The measurement of absolute M1 transitions thus provide strong constraints on the structure of the interaction. Branching ratios are rather insensitive on the precise structure of the hamiltonian, and we have obtained predictions that can be tested directly with experiment.

---

* K.V.I., Groningen
** Brookhaven National Laboratory

1. D. Bohle et al., Phys. Lett. 137B, 27 (1984); Phys. Lett. 148B, 260 (1984).
2. F. Iachello, Nucl. Phys. A358, 89C (1981).

INELASTIC PROTON SCATTERING AS A TEST OF THE NEW COLLECTIVE "CURRENT" M1 MODE IN DEFORMED NUCLEI

J.A. Carr*, F. Petrovich*, R.J. Philpott*, M. Threapleton*, O. Scholten, and H. McManus**

The electromagnetic M1 operator has both spin and current components and nuclear magnetic dipole transitions which proceed predominantly through either the spin or current part are conveniently classified as "spin" or "current" excitations, respectively. Partly because the interaction between bound nucleons is more effective in building spin correlations than current correlations in nuclei, and partly because the electromagnetic spin coupling is somewhat stronger than the current coupling, the majority of known M1 excitations are of the "spin" type although examples of both types have been discussed in the literature.[1] Quite recently there has been considerable theoretical interest in a collective "current" M1 mode peculiar to deformed nuclei.[2-8] The state of interest is the isovector counterpart of the spurious, isoscalar $K=1^+$ state in deformed nuclei corresponding to the motion of the protons and neutrons of the nucleus in the angle between their respective symmetry axes as the nucleus as a whole undergoes rotation. Evidence for substantial M1 strength near the excitation energy predicted for this collective current mode has been obtained in a recent low momentum transfer, backward angle electron scattering experiment on the nucleus ^{156}Gd.[9,10] Further electron scattering and resonance fluorescence work, as yet unpublished, provides additional evidence for this new collective mode in other nuclei.[11]

Electromagnetic studies alone cannot unambiguously establish that an unnatural parity dipole transition is a "current" excitation. For this reason we have studied the excitation of this state by protons with E_p=200 MeV. In contrast to electrons, at low momentum transfer the 1^+ levels are almost exclusively excited through the spin operator.

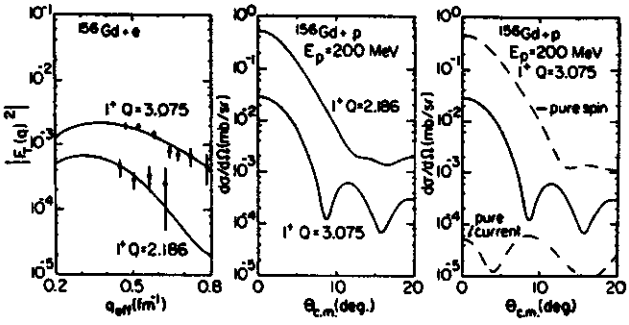

Fig. 1. The predicted transverse-magnetic electron scattering form factors (left) and (p,p') differential cross sections (center) are displayed with the effects of distortion included. For electron scattering we plot the experimental data corrected for Coulomb distortion versus q_{eff} so we can compare them to a plane wave form factor. The rightmost panel contrasts the predicted (p,p') cross section for the 3.075 MeV state calculated from the IBA wave function (solid curve) to those computed from pure spin (top) and pure current (bottom) transition densities.

In Fig. 1 the calculated form factor for electron scattering and cross section for proton scattering is displayed for two known 1^+ levels in ^{156}Gd. The level at Q=2.186 is a 2 q.p. level and is expected to be much stronger excited in proton scattering than the collective current M1 mode and Q=3.075 MeV. In electron scattering the reverse appears to be the case. A combination of electron and proton scattering data thus provide a separate determination of the spin and the current transition matrix element.

* Florida State University
** Department of Physics and Astronomy, MSU

1. L.W. Fagg, Rev. Mod. Phys. 47, 683 (1975) and references cited therein.
2. T. Suzuki and D.J. Rowe, Nucl. Phys. A289, 461 (1977).
3. N. Lo Iudice and F. Palumbo, Phys. Rev. Lett. 41, 1532 (1978); Nucl. Phys. A326, 193 (1979).
4. F. Iachello, Nucl. Phys. A358, 89c (1981).
5. A.E.L. Dieperink, Prog. Part Nucl. Phys. 9, 121 (1983).
6. M. Sambataro, O. Scholten, A.E.L. Dieperink, and G. Piccitto, Nucl. Phys. A423, 333 (1984).
7. D.R. Bes and R.A. Broglia, Phys. Lett. 137B, 141 (1984).
8. H. Kurasawa and T. Suzuki, Phys. Lett. 144B 141 (1984).
9. D. Bohle et al., Phys. Lett. 137B, 27 (1984).
10. A. Richter, Proc. Intl. Symp. on Electro-Magnetic Properties of Atomic Nuclei, ed. H. Horie and H. Ohnuma (Tokyo Institute of Technology, Tokyo, 1984) p. 202.
11. A. Richter, private communication.

HARTREE-FOCK CALCULATIONS OF LIGHT NEUTRON-RICH NUCLEI

H. Sagawa and H. Toki

Stimulated by recent measurements of nuclear radii and life times of light neutron-rich nuclei,[1,2] we have performed the Hartree-Fock calculations of nuclear radii, binding energies, and density distributions of He-, Be-, C- and O-isotopes. As for the Skyrme interaction, there are various parameter sets. We select two parameter sets SIII[3] and SkM[4] to the present calculations. The main difference of two interactions is the power of the density-dependence. The SIII has a linear power of the density-dependence force, while SkM has a lower power of density-dependence 1/6. They induce different nuclear matter compression moduli for two interaction, i.e., K_∞=356 MeV for SIII and 218 MeV for SkM. The former reproduces well the binding energies of many nuclei, on the other hand, the density distributions of nuclei are obtained better by the interaction SkM than those having higher compression moduli.

In our calculations, the open-shell nuclei are treated by filling the single-particle states in the order of the calculated single-particle energies. Thus, the occupation probability of the single-particle state is always one except the last occupied state. Fig. 1 shows the radii of the He-isotopes as a function of mass number. The experimental values obtained by the secondary beam method[1] are denoted by dots with error bars. We plot in Fig. 1 a mean radii $\bar{r}$ obtained by taking the average of the square radii of protons and neutrons $\bar{r}^2=(Zr_p^2+Nr_n^2)/A$ since the reaction cross section will reflect both proton and neutron density distributions. The two results obtained by SIII and SkM interactions are similar to each other in the cases of A=6 and 8, and agree with the experimental results. The experimental values except ^{4}He follow a simple formulae $r=1.2A^{1/3}$ m. We note the radius of ^{10}He is increased much from that of ^{8}He. This is because the single particle state $1p_{3/2}$ for

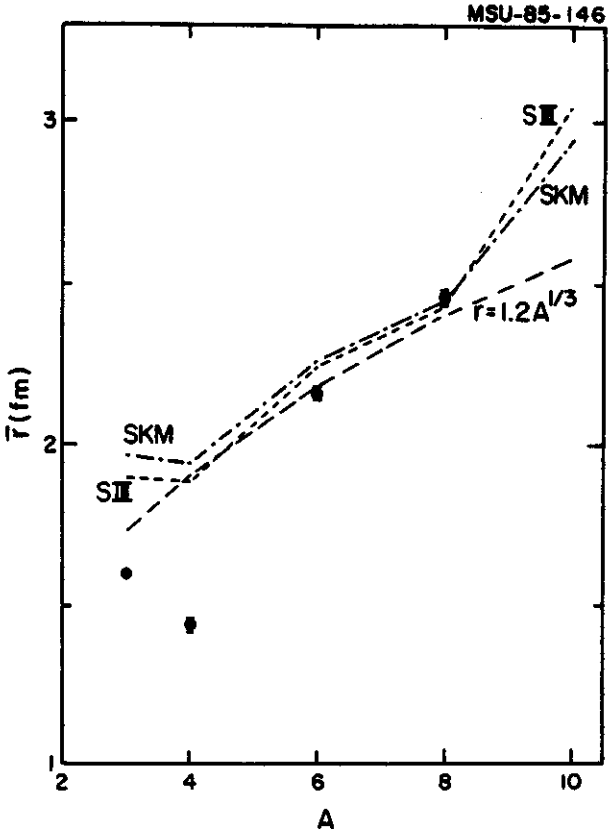

Fig. 1. The mass radii $\bar{r}^2=(Zr_p^2+Nr_n^2)/A$ of the He-isotopes calculated by the Hartree-Fock approximations with the Skyrme interactions SIII (dotted line) and SkM (dotted-dashed line) as a function of the mass number. The experimental data are taken from Ref. 1.

neutron is very weakly bound. The calculated binding energies, especially using the SIII interaction, show also good agreements with experimental data.

We showed in Fig. 2 the binding energies of Be-, C- and O-isotopes together with the empirical ones as a function of the neutron number. The calculated results reproduce remarkably well the N-dependence of the binding energies of all three isotopes. In the case of ^{8}Be, the experimental energy is somewhat larger

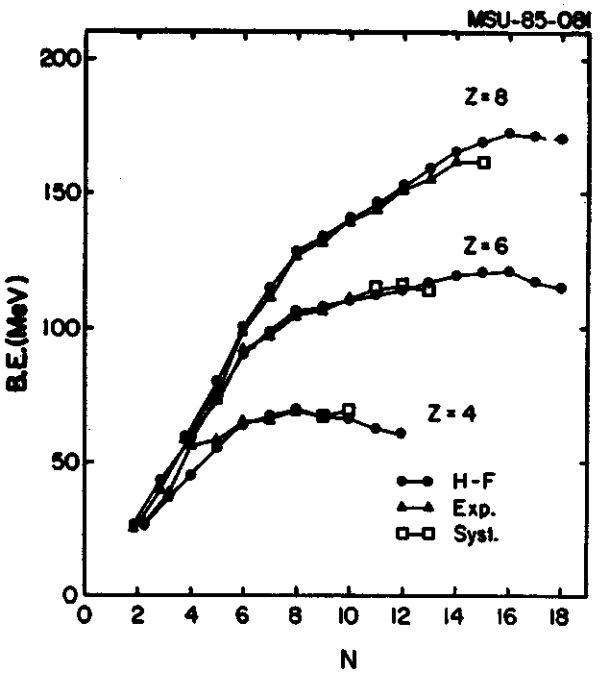

Fig. 2. The H-F and experimental binding energies of Be-, C- and O-isotopes with respect to the neutron number N. The SIII interaction is used in the H-F calculations. The H-F energies are denoted by the open circles, while the experimental ones correspond to the black ones. The triangles are obtained by the empirical systematics in Ref. 5.

than the H-F one because of the α-cluster correlation. It is interesting that both the H-F and the experimental binding energies are independent to the proton number Z in nuclei with small N. Namely, the binding energies are almost same for the following each pair: (^{6}Be, ^{8}C), (^{7}Be,^{9}C), (^{8}Be,^{10}C),(^{10}C,^{12}O) and (^{11}C,^{13}O).

We can see in Fig. 4 that the nuclei ^{20}C, ^{22}C, ^{22}O and ^{24}O might be a long-lived nuclei with a typical life time of β-decay (10 ms -100 ms). The odd neutron-rich nuclei are unlikely to be long-lived nuclei because of the odd-even mass difference (the pairing effect which is not taken into account in the H-F calculations). In a comprehensive study of the nuclear mass,[6] ^{20}C and ^{22}O are also identified as the long-lived nuclei with the half-lives $T_{1/2}$=50 ms and $T_{1/2}$ =100ms, respectively, although their binding energies have not yet been determined experimentally. It might be an interesting challenge to study masses and lifetimes of these nuclei experimentally.

1. I. Tanihata et al, preprint (Berkeley, 1984)
2. J. Stevenson et al., Phys. Rev. Lett. 53, 2544 (1984)(1985)
3. D. Vautherin and D. M. Brink, Phys. Rev. C5, 626 (1972)
4. H. Krivine et al., Nucl. Phys. A336, 155 (1980)
5. A. H. Wapstra and K. Boss, Atomic Data and Nuclear Data Tables 19, 177 (1977)
6. K. Takahashi et al., Atomic Data and Nuclear Data Tables 12, 101 (1973)

THE GIANT-DIPOLE AND SPIN-DIPOLE RESONANCES: A COEXISTENCE PROBLEM

H. Sagawa and B. Castel*

Spin-dipole resonances are excited through the transition operators

$$\hat{T}^{SP}_{\lambda\mu}=\sum_i r_i^{l=1}[Y_{l=1}(\hat{r}_i)\times\sigma_i]_{\lambda\mu}\cdot\tau, \quad \lambda=2^-, 1^-, 0^-, \quad (1)$$

in intermediate-energy hadron scattering at forward angle (θ=5-15°). One multipole of the spin-dipole states has the same angular momentum and parity $J = 1^-$ as the giant-dipole resonance, itself induced by the operator

$$T^{NS}_{\lambda\mu} = \sum_i r_i^{\lambda=1} Y_{\lambda=1}(\hat{r}_i)\cdot\tau, \quad \lambda=1^-, \quad (2)$$

in electron scattering or photoreaction. In a shell-model study of $J=1^-$ states in ^{16}O,[1] the results, displayed in Table 1, indicate that the central part of the interaction alone yields one state at 21.8 MeV exhausting the total S=0 strength while another state at 19.8 MeV accounts for 95% of the total transition strength for the spin-dependent operator. When

Table 1. Energies and transition strengths of T=1, $J=1^-$ states in ^{16}O calculated with a Sussex interaction.

E(MeV)	B(E1;S=0)[%]	B(E1;S=1)[%]
	Vc(central) only	
15.2	0.	5.
16.1	0.	0.
17.4	0.	0.
19.8	0.	95.
21.8	100.	0.
	$V_c + V_{LS} + V_T$	
11.7	0.	4.
17.6	1.	17.
19.3	4.	9.
21.4	88.	1.
27.1	7.	68.

the two-body spin-orbit and the tensor interactions are included in the calculation, the spin-dependent strength is largely split out, but the spin-independent transition strength still remains concentrated in one state. This difference can be understood by the following intuitive arguments of the effective interactions.

The tensor interaction can be given in the form

$$V_T(r) = F(r)\{[\sigma_1\times\sigma_2]^{(2)}\times[r^2Y_2(\hat{r})]^{(2)}\}^{(0)}. \quad (3)$$

Taking the expansion formula of the solid spherical harmonics $r^2Y_{2\mu}(\hat{r})$ for two separate coordinates, we can express the tensor interaction in terms of the spin-dipole operators[2]

$$V_T(r) = F(r)\sum_\lambda (-)\frac{1}{6}\sqrt{4\pi}\,[\tfrac{10}{3}]^{1/2}\begin{Bmatrix}2\sqrt{5}\\-\sqrt{15}\\1\end{Bmatrix} \quad (4)$$

$$\times\{r_1[\sigma_1\times Y_1(\hat{r}_1)]^{(\lambda)}\times r_2[\sigma_2\times Y_1(\hat{r}_2)]^{(\lambda)}\}^{(0)}, \quad \lambda^\pi=\begin{matrix}0^-\\1^-\\2^-\end{matrix}$$

The spin-orbit two-body operator L.S is also proportional to the spin-dipole operator as follows

$$L\cdot S\propto r_1\{[\sigma_1\times Y_1(\hat{r}_1)]^{(1)}\times p_2\}^{(0)}$$
$$+ r_2\{[\sigma_2\times Y_1(\hat{r}_2)]\times p_1\}^{(0)} \quad (5)$$

In Eq. (5), the spin-dipole operator can couple to $\lambda\pi=1^-$ only. We can now see from Eqs. (4) and (5) that the direct two-body matrix element of the tensor and spin-orbit forces is finite only for the spin-dependent configurations. Spin-independent excitations receive contributions from exchange matrix elements which are in general several times smaller than the direct ones. Thus, the spin-independent excitations are practically insensitive to tensor and spin-orbit forces, while the spin-dependent ones are

greatly affected both in excitation energies and transition strengths. We should note that since the spin-isospin channel of the central interaction is repulsive, the effects of the tensor and central forces would interfere constructively since F(r) as given in Eq. (4) is repulsive. In fact we can see from Table 1 that the average excitation energy with the full interaction is 4.2 MeV higher than that with the central interaction alone.

One interesting feature of the results displayed in Table 1 is that the giant dipole state always has a very small spin transition strength with or without the tensor and the spin-orbit forces. Since ^{16}O is a closed-core in both LS and jj coupling, the total spin is zero in the ground state. Thus the giant-dipole state which has no intrinsic spin-component cannot have any matrix element for the spin-dependent operator. It is also well-known that ^{12}C is not a good jj coupling core, but remains close to the LS coupling core. In this sense, the giant-dipole state in ^{12}C would also not have large transition strength for the spin-dependent operator which is consistent with the small cross sections observed in (p,n) (Ref. 2) and pion reactions (Ref. 3) in the vicinity of the GDR. Similar arguments might be true also for other collective states 2^+, 3^- and so on.

---

*Queen's University at Kingston

1. B. Castel and A.G.M. van Hees, Phys. Rev. C28, 2571 (1983);B. Castel, A.G.M. van Hees, and L. Zamick, Nucl. Phys. A415, 30 (1984).
2. C. Gaarde et al., Nucl. Phys. A422, 189 (1984).
3. L.C. Bland et al., Phys. Rev. Lett., to be published.

THERMAL PROPERTIES OF FINITE NUCLEAR SYSTEM IN THE CONSTRAINED HARTREE-FOCK APPROXIMATION

H. Sagawa and H. Toki

Thermal properties of nuclei have been of great interest recently in the context of the interpretation of data from intermediate-energy heavy-ion experiments.[1,2] The saturation properties of nuclear systems at finite temperatures are particularly interesting in relation to the giant compression mode[3] and the liquid-gas phase transition.[1,2,4] So far, these problems have been discussed in terms of nuclear matter calculation and the Thomas-Fermi approximation.[1-4]

In order to study the nuclear compression modulus at finite-temperature and also the equation of state of the finite nucleus, we must perform a constrained H-F calculation. Until now, such constrained H-F calculations have been done only at zero temperature.[5,6] In this work, we discuss results of constrained H-F calculations at several finite-temperatures. We have chosen medium and heavy nuclei ^{90}Zr and ^{208}Pb for this study.

The Hartree-Fock theory at finite-temperature can be formulated by considering the variation of the thermodynamical potential with respect to the grand canonical partition function of the system.[5,7] The variation of the thermodynamical potential with respect to $f_i(T)$ gives the condition,

$$f_i(T) = 1/\{1 + \exp[(h_i - u)/T]\} \qquad (1)$$

where h_i is the H-F Hamiltonian density. Small changes of the trial wave functions around the occupation probability given by Eq. (1) leads to the H-F equation at finite temperature. The H-F equation should be solved self-consistently together with the subsidiary condition (1). In order to study the dilute system at finite temperature, we take a constrained-Hamiltonian for the density,

$$h_i'(\rho) = h_i(\rho) - \lambda\rho(\vec{r}) \qquad (2)$$

where λ is the Lagrange-multiplier.

The H-F coupled equations (1) and (2) were solved by the Numerov algorithm in the coordinate space. The continuum states are calculated as discrete states in a large sphere with radius R=15 fm for ^{90}Zr and R=18 fm in ^{208}Pb, respectively. We should notice that the entropy and the rms radius above T=7 MeV are sensitive to the radius R. If we change the value R from 18 fm to 20 fm, the entropy and the rms radius increase by 10-15% and 5-8%, respectively, above T=7 MeV. While the changes are less than 5% below T=6 MeV. We take 30 (40) single-particle states for proton and neutron configurations in the H-F calculations of ^{90}Zr (^{208}Pb). As we will see later, these configuration spaces are not large enough to estimate properly the entropy at temperatures above T=4 MeV. However, they seem to be adequate for the calculations of the H-F density and potential. We take into account the single-particle states until the N=15 (N=2n+1) major shell in the calculations of the entropy and the chemical potential.

The saturation curves of the free energy $F=\langle\hat{H}\rangle-TS$ versus the rms radius for the mass distribution $r_m=\sqrt{\langle r^2\rangle_m}$ are shown in Fig. 1 for ^{90}Zr and ^{208}Pb. Since r_m is a smooth and unique function of the λ-value at each temperature, we can use the rms radius r_m instead of λ as a physical parameter for studying saturation properties. We summarize various properties at the saturation point ($\partial(F/A)/\partial r_m=0$) for different temperatures in Table 1. The saturation point becomes shallower at higher temperature, and the free energy F has no minimum above T=6 MeV in ^{90}Zr and above 7 MeV in ^{208}Pb. This indicates that these nuclei are unstable above these temperatures. The rms radii increase very slowly until T=4 MeV, but show a sudden change at T=6 MeV both in ^{90}Zr and ^{208}Pb. This rapid change in the rms radius is

also found in the calculation of Ref. 8 for ^{208}Pb. We find that an increase in the temperature also decreases K_A. This low compression modulus and large rms radius are both induced by the reduction in the depth of the saturation minimum at high temperatures as

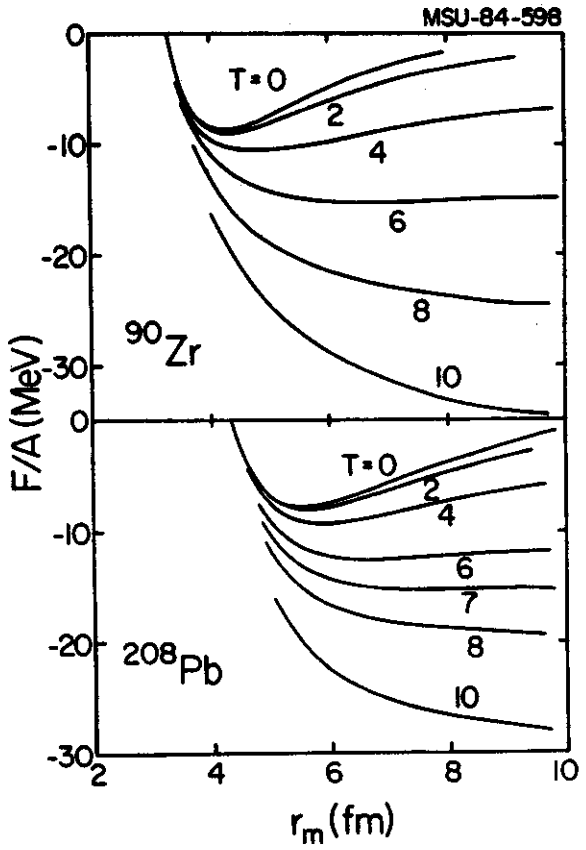

Fig. 1. The free energies of ^{90}Zr and ^{208}Pb as a function of the rms radius r_m at various temperatures.

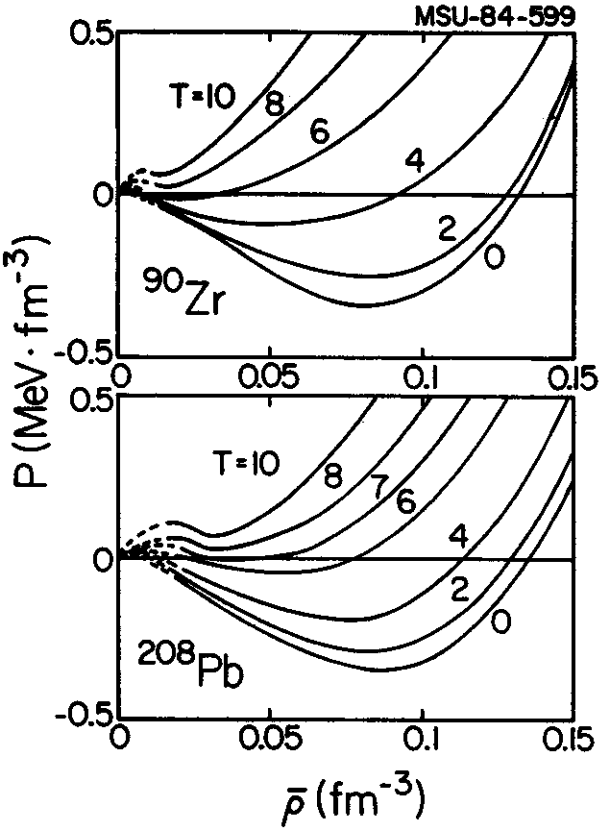

Fig. 2. The equation of state in ^{90}Zr and ^{208}Pb. The pressure is evaluated by Eq. (3). The dashed curve is drawn as an extrapolation of the solid curve above the density $\bar{\rho}$=0.01 fm^{-3}.

Table 1 Saturation properties of ^{90}Zr and ^{208}Pb. The free energy and the thermal excitation energy are defined by $F=\langle\hat{H}\rangle - TS$ and $E^*=\langle\hat{H}\rangle_T - \langle\hat{H}\rangle_{T=0}$, respectively.

	T(MeV)	S	F/A(MeV)	E^*(MeV)	μ_p(MeV)	μ_n(MeV)	r_m(fm)	K_A(MeV)	$\hbar\omega$(MeV)
^{90}Zr	0.	0.	-8.74	0.	-5.74	-9.87	4.23	143.4	18.2
	2.	30.7	-9.03	34.9	-6.43	-10.07	4.27	121.0	16.6
	4.	89.5	-10.53	156.7	-7.34	-11.30	4.87	58.5	10.1
	6.	211.4	-15.28	685.7	-9.74	-13.45	7.03	43.5	6.0
^{208}Pb	0.	0.	-7.86	0.	-4.04	-6.17	5.52	147.	14.1
	2.	65.3	-8.09	81.3	-4.79	-7.39	5.60	121.	12.6
	4.	152.4	-9.35	298.8	-5.50	-8.70	5.78	81.	10.0
	6.	313.2	-12.81	903.1	-7.15	-10.75	6.75	39.	5.9

is shown in Fig. 1.

In order to study the equation of state, we introduce the average density, related to the rms radius by $\bar{\rho}=3A/[4\pi(5r_m^2/3)^{3/2}]$. Defining the nuclear volume by $V=A/\bar{\rho}$, we can evaluate the pressure from the equation,

$$P = -\frac{\partial(F/A)}{\partial(V/A)} = \bar{\rho}^2 \frac{\partial(F/A)}{\partial\bar{\rho}} \qquad (3)$$

The isothermal equation of state in ^{90}Zr and ^{208}Pb are shown in Fig. 2 up to T=10 MeV. We plot the equation of state at very low density as a smooth extension of our results down to $\rho=0.01$ fm^{-3}. Concerning the critical temperature of the liquid-gas phase transition,[1,2,4] signaled by the disappearance of the local minimum in the P-$\bar{\rho}$ diagram, we are not able to provide a definite number due to the difficulties in solving the H-F equations at very low densities. However, the extrapolation of the available calculated results for ^{90}Zr and ^{208}Pb indicate a critical temperature of $T_c\simeq$10-15 MeV and a corresponding density of $\bar{\rho}_c\simeq$0.01-0.02 fm^{-3}.

1. M. W. Curtin et al, Phys. Lett. 123B, 289 (1983)
2. A. D. Panagiotou et al., Phys. Rev. Lett. 62, 405 (1984)
3. J. Meyer et al, Phys. Lett. 133B ,279 (1983)
4. G. Sauer et al, Nucl. Phys. A264, 221 (1976)
5. S. K. M. Wong et al, Nucl.Phys. A169, 294 (1971)
6. W. H. Bassichis et al, Nucl. Phys. A263, 379 (1976)
7. D. J. Thouless, The quantum mechanics of many-body systems (Academic Press, New York, 1972)
8. P. Bonche et al, Nucl. Phys. A427, 278 (1984)

ANOMALOUS E1 TRANSITIONS NEUTRAL-WEAK CURRENTS IN NUCLEI?

Wm. C. McHarris and John O. Rasmussen[a]

With mounting evidence for parity-violating effects in atoms caused by the interference of neutral-weak and electromagnetic currents [1], one is tempted to look for similar effects in nuclei. The major difficulty is that neutral-weak ("neutral-β") transitions would have to compete with γ transitions, which are intrinsically faster by factors in the vicinity of 10^9. Parity-violating effects would be the most clear-cut signatures, but, in addition, the first place to search would be where structure effects hinder γ transitions but perhaps not the competing β transitions.

The so-called anomalous E1 transitions in deformed heavy nuclei [2] make good possibilities for scrutiny. These transitions are regularly hindered by factors of 10^5 or more, and in at least one case by as much as 10^7. In addition, the conversion coefficients for $s_{1/2}$ and $p_{1/2}$ electrons are anomalously large, at times by factors of several hundred. To a first approximation, the greater the degree of hindrance, the larger the anomalous conversion coefficient. In the past these have been explained, in a more or less ad hoc fashion, by considering the penetration of the electrons into the nucleus and expanding the electronic wave-functions within the nuclear radius [3].

An alternate view would be the following: In larger nuclei first-forbidden β transitions are becoming increasingly enhanced, both because of the larger nuclear radii themselves and because of the relativistically-enhanced source-velocity effects; thus, by the time the actinide nuclei are reached, these first-forbidden transitions are considerably faster than normal allowed transitions. A first-forbidden β transition would compete with an E1 γ transition, and for the "anomalous" E1 transitions in the actinides, it is conceivable that much of the intrinsic difference in rates between weak and electromagnetic interactions has been accounted for. Specifically, "neutral-β decay" would masquerade to first order as the emission of conversion electrons -- there would be a nucleon-electron interaction at both the incoming and outgoing vertices of the Feynman diagrams, making this in effect a kind of electron scattering. Is it possible that a portion of the excess electron intensity attributed to the electromagnetic interaction in these anomalous E1 transitions originates, in fact, from neutral-β decay?

The amplitude for low-energy neutral-weak coupling between an electron and a proton or a neutron can be written respectively as [4]:

$$\underline{M}(e,p) = -(G_F/2\sqrt{2})\bar{u}_e'\gamma^\mu(1-4\sin^2\theta_W-\gamma_5)u_e$$

$$\times\ \bar{u}_p'\gamma_\mu(1-4\sin^2\theta_W-1.25\gamma^5)u_p$$

and

$$\underline{M}(e,n) = (G_F/2\sqrt{2})\bar{u}_e'\gamma^\mu(1-4\sin^2\theta_W-\gamma_5)u_e$$

$$\times\ \bar{u}_n'\gamma_\mu(1-1.25\gamma^5)u_n$$

Thus, for the expected values of the Weinberg angle near 30°, neutrons, but not protons, contribute coherently to the amplitude, enhancing the possible effect in very heavy nuclei.

We have been performing preliminary calculations and find it likely that neutral-β decay does contribute to the observed electron excess in some of these transitions. (This means that neutral-weak currents were, in effect, probably "observed" some two decades ago -- but, of course, they were not recognized for what they were, since no one was looking for such a thing.) Much remains to be done -- in

particular, investigating the possible parity-violating and interference effects, such as recoil correlations.

Prof. Eugene Commins has helped us greatly with his insights, for which we thank him.

---

a. Lawrence Berkeley Laboratory

1. P. S. Drell and E. D. Commins, Phys. Rev. Lett. 53, 968 (1984); see also the review article by E. N. Forston and L. L Lewis, Physics Reports 113, 289 (1984).
2. F. T. Porter, I. Ahmad, M. S. Freedman, J. Milsted, and A. M. Friedman, Phys. Rev. C 10, 803 (1974).
3. S. G. Nilsson and J. O. Rasmussen, Nucl. Phys. 5, 617 (1958).
4. E. D. Commins and P. H. Bucksbaum, Weak Interactions of Leptons and Quarks, Cambridge Univ. Press (1983), Chaps. 4 and 9.